

## MICROSTRUCTURE AND CORROSION BEHAVIOUR OF ALUMINUM FLY ASH COMPOSITES

J. Bienias<sup>\*</sup>, M. Walczak, B. Surowska, J. Sobczak<sup>a</sup>

Department of Materials Engineering, Lublin University of Technology 36 Nadbystrzycka St, 20-618 Lublin, Poland

<sup>a</sup>Foundry Research Institute, Light Metal Division, 73 Zakopiańska St, 30-418 Cracow, Poland

The microstructural characteristics of aluminium matrix AK12 composites containing of fly ash particles (precipitator), obtained by gravity and squeeze costing techniques, pitting corrosion behaviour and corrosion kinetics are presented and discussed. It was found that: (1) in comparison with gravity casting, squeeze casting technology is advantageous for obtaining higher structural homogeneity with minimum possible porosity levels, good interfacial bonding and quite a uniform distribution of reinforcement, (2) fly ash particles lead to an enhanced pitting corrosion of the AK12/9.0% fly ash (75-100  $\mu\text{m}$  fraction) composite in comparison with unreinforced matrix (AK12 alloy), and (3) the presence of nobler second phase of fly ash particles, cast defects like pores, and higher silicon content formed as a result of reaction between aluminium and silica in AK12 alloy and aluminium fly ash composite determine the pitting corrosion behaviour and the properties of oxide film forming on the corroding surface.

(Received April 11, 2003; accepted May 8, 2003)

*Keywords:* Aluminium, Corrosion kinetics, Fly ash, Metal-Matrix Composites, Microstructure, Pitting corrosion

### 1. Introduction

Aluminium-fly ash (ALFA) composites have been developed in recent years. Fly ash is a particulate waste material formed as a result of coal combustion in power plants. The use of fly ash as a filler or reinforcement for aluminum alloys, called Metal Matrix Composites (MMC's), is, therefore, very desirable from an environmental standpoint. Fly ash forms at temperatures in the range of 920-1200 °C and is collected as precipitator ash (solid particles) and cenospheres (hollow microspheres) that float on collection ponds [1,2]. Cenosphere has a low density of about 0.6 g cm<sup>-3</sup>, and can be used for the synthesis of ultra-light composites materials, whereas precipitator fly ash has a density in the range of 2.0-2.5 g cm<sup>-3</sup>. It can improve various properties of selected matrix materials, including stiffness, strength, and wear resistance [3-5].

Fly ash contains fine mainly silica and alumina with minor amounts of calcium and magnesium oxides [6]. Production of aluminium alloy-fly ash composite material is difficult due to the poor wettability of fly ash and its low weight. The introduction of fly ash into liquid metal for making gravity castings often does not result in a uniform distribution of fly ash particles in the alloy structure [5]. However, further re-melting of the composite material combined with squeeze casting has been found to improve the distribution in aluminium-fly ash castings. Initial investigations employing a squeeze casting process (the application of external pressure on the molten metal) for aluminum-fly ash MMC's have also demonstrated many advantages of this technique [7-9] such as: (a) better compatibility between the metal matrix and the fly ash particles, (b) a more improved

---

\*Corresponding author: bienio@archimedes.pol.lublin.pl

structure of the matrix alloy, (c) filling of some hollow particles of the fly ash with metal, and (d) pressure activation of the fly ash-metal interface.

Incorporation of a second phase into a matrix material can enhance the physical and mechanical properties of the latter, thereby significantly changing its corrosion behaviour. The corrosion behaviour of metal-matrix composite is determined by several factors such as the composition of the alloy, the matrix microstructure, the dispersoid and the matrix, and the technique adopted for preparing the composite. A very small change in any one of these factors can seriously affect the corrosion characteristics of the metal [10-15]. Aluminium-fly ash composites offer many potential applications particularly for internal combustion engine pistons and brake rotors due to their density and high mechanical properties [3,16]. Additionally, the results of hardness and electrical conductivity of the investigated composites show [5] that uniformly dispersed reinforcing phases and adequate machinability are possible. From both an economical and environmental standpoint the use of fly ash for reinforcing aluminium alloys is extremely attractive due to its waste material character and expected low costs of production [1,5].

The published literature on advanced materials, such as Aluminium Fly Ash (ALFA) composites, is rather limited and is primarily concerned with applications of fly ash particles for synthesis of these materials. There is also a lack of information on the influence of fly ash particles on the susceptibility of ALFA composites to corrosion. Therefore, it was thought worthwhile to study: (1) the microstructural characteristics of aluminium composites reinforced with fly ash particles, and (2) the relationships between the composite microstructure and corrosion behaviour in a typical corrosive environment. The present work is dedicated to such an investigation.

## 2. Experimental

AK12 (AlSi12CuNiMg) aluminium-silicon base alloy (eutectic silumin with solidification range 562-520 °C) was used as the metal matrix. Chemical composition of AK12 alloy is given in Table 1. Fly ash particles (precipitator) used to synthesize the composite material was received from Dayton Power and Light Company (DP&L, USA). The composition of the fly ash particles is given in Table 2. Before the synthesis of the composite material, fly ash particles were cleaned by magnetic separation and then sifted to the size fractions: 53-75 µm and 75-100 µm. Larger particles of fractions 100-150 and 150-250 µm were not demagnetized.

Table 1. Chemical composition limits of metal matrix, wt. % (according to Polish Standard PN-76/H-88027).

Alloying elements				Impurities max.			
Si	Cu	Mg	Ni	Fe	Zn	Mn	Ti
11.3-13	0.8-1.3	0.8-1.5	0.8-1.1	0.6	0.2	0.2	0.1

Table 2. Chemical composition of fly ash particles (data from DP&L, in wt%).

SiO <sub>2</sub>	Al <sub>2</sub> O <sub>3</sub>	Fe <sub>2</sub> O <sub>3</sub>	K <sub>2</sub> O	CaO	MgO	TiO <sub>2</sub>	Na <sub>2</sub> O	P <sub>2</sub> O <sub>3</sub>	Mn <sub>2</sub> O <sub>3</sub>	SrO
55.9	30.2	5.4	2.7	1.3	1.0	1.6	0.2	0.4	0.1	0.1

The fly ash particles were stirred under an argon cover in the AK12 molten alloy after being initially preheated up to 800 °C for 22 h in small graphite crucibles. The metal matrix was melted in a graphite crucible located inside a resistance furnace. The amount of the metal used was always 10.20 kg. The amount of fly ash was chosen according to its desired final concentration. Before and during stirring, some magnesium chips in the amount of 0.98 % were added to the molten slurry. Final

concentrations of fly ash in the composites were 3.7 wt.% and 9.0 wt.%. The temperature of the metal was 780 °C before mixing, 760 °C during mixing and the suspension was poured at 750 °C. The composites for the study were then synthesized by gravity and squeeze casting techniques.

The corrosion resistance experiments were carried out by accelerated electrochemical studies using the potentiodynamic method on AK12/9.0% fly ash (75-100 µm fraction) composite after gravity casting and its unreinforced matrix. The potentiodynamic measurements were made in the 3.5 wt.% NaCl aqueous solution of pH 7.0 at 25 °C, with Pt counter-electrode. Samples with an active surface of 1 cm<sup>2</sup> were mechanically polished with diamond paste with a granularity of 3 µm, then thoroughly rinsed with distilled water and placed, when wet, in the measurement vessel. When the corrosion potential  $E_{\text{corr}}$  (after 30 min) was achieved, anodic polarization curves were recorded with an automatic potential shift at a rate of 10<sup>-3</sup> V. Polarization was started at a potential of -1600 mV shifting the potential towards the anodic side till a clear increase in the current density was observed. Then the direction of polarization was changed and the measurements were recorded again on the cathodic side. The potential was controlled with an EG-20 type generator, EP-20 potentiostat and a PC equipped with reference to a saturated calomel electrode.

The corrosion behaviour of the materials was studied further by immersion tests. Samples in the shape of half-disc specimens of 18 mm radius and 3 mm thickness were cut from the composites and matrix alloy. They were ground to 800 grit and then cleaned with acetone, dried, weighed and immersed in an unstirred solution of 3.5 wt.% NaCl (pH 7.0) in distilled water exposed to atmospheric air. The test were performed at room temperature (22 °C). The solution-to-specimen area ratio was about 1 ml mm<sup>-2</sup>. To avoid crevice corrosion, the specimens were suspended in the solution with a plastic string passing through a 2 mm diameter hole through them. Every 5 days the specimen were first mechanically cleaned with a brush made of plastic strings, and then chemically cleaned in a solution of 2.0 wt.% chromic acid and 3.5 wt.% phosphoric acid at 98 °C for 10 s, dried and weighed. The accuracy in the determination of weight was ± 0.05 mg.

The microstructure was studied using an optical microscope (ZEISS model) and a scanning electron microscope (Hitachi S-3500N).

### 3. Metal matrix microstructure

Good retention of fly ash particles was clearly seen in the microstructures of AK12/fly ash composites. This feature is shown in Fig. 1. Coagulation of some fly ash particles and development of some primary silicon single crystals in the vicinity of fly ash colonies are also seen in this figure. A characteristic feature of our cast particulate reinforced composites is a considerable amount of porosity or sponginess in the structure, as shown in Fig. 2. Usually, the porosity is close to the particle-matrix interface.

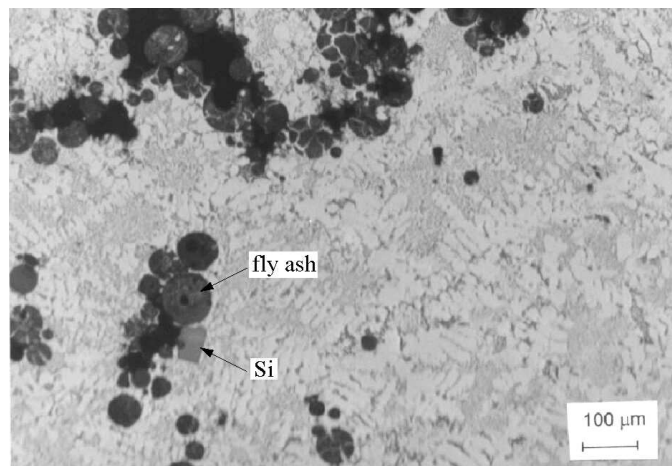


Fig. 1. Microstructure of ALFA AK12/9.0% fly ash (53-75 µm fraction) composite after gravity casting (as cast). Primary Si single crystals are also seen.

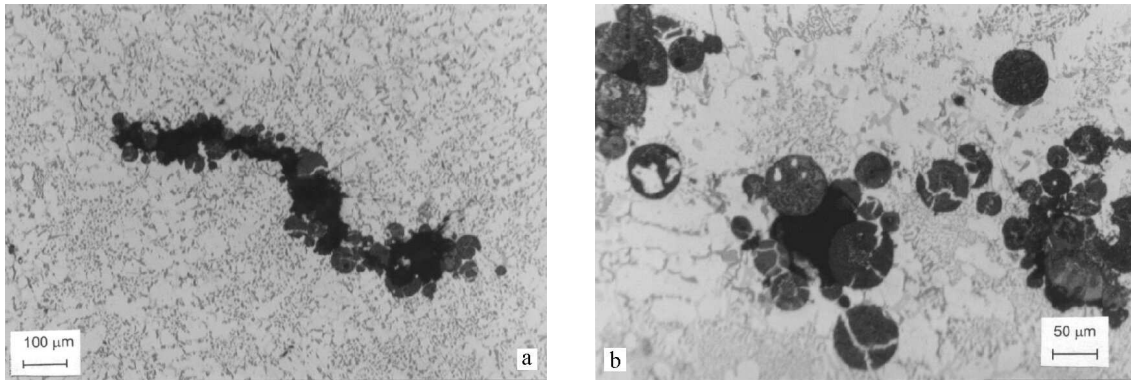


Fig. 2. Microstructure of ALFA AK12/3.7% fly ash (53-75  $\mu\text{m}$  fraction) composites after gravity casting: (a) characteristic chain of porosity surrounded by fly ash particles after heat treatment and (b) agglomerates of fly ash particles in the neighbourhood of pores in a sample without heat treatment.

After squeeze casting, the fly ash particles are bonded very well with the base metal matrix. This feature may be seen in Fig. 3. Each squeeze cast composite structure may be seen to be relatively free from porosity. Fly ash particles are quite uniformly distributed in the structure. Hollow fly ash particles composing cenospheres (Fig. 3b) as well as some cenospheres filled with matrix metal are observed (Fig. 4).

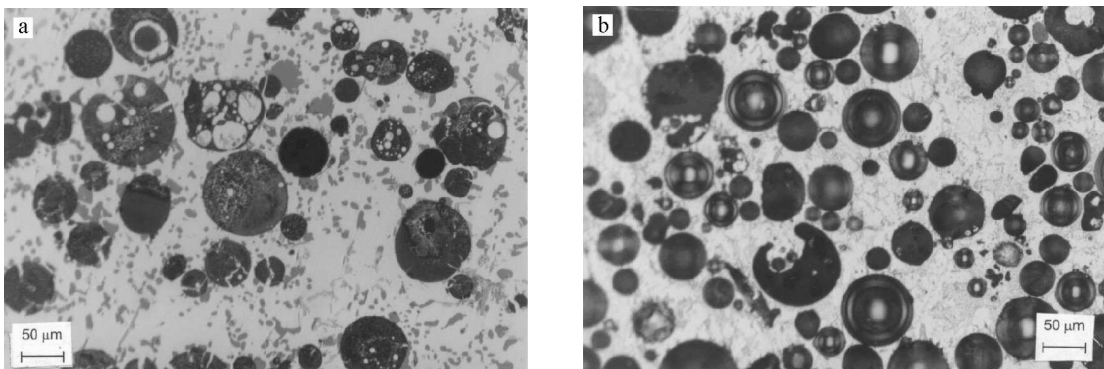


Fig. 3. Typical examples of microstructure of ALFA AK12/9.0% fly ash (53-75  $\mu\text{m}$  fraction) composite after squeeze casting (as cast). Quite uniform distribution of fly ash particles in the structure and good bond between particles and the matrix may be seen in these figures. Cenospheres with filled fly ash particles without porosity may be seen in (b).

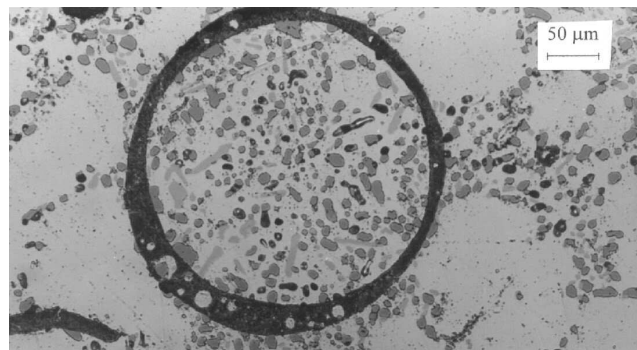


Fig. 4. Microstructure of ALFA AK12/9.0% fly ash (75-100  $\mu\text{m}$  fraction) composite after squeeze casting (heat treated). Large unsifted cenosphere contains excess amount of silicon phase.

An important feature of the aluminium alloy composite containing fly ash particles is their distribution and interface between reinforcement and matrix [5]. In the case of composites after gravity casting, occurrence of agglomerations can be caused by a characteristic limitation of the stirring technique. Porosity located in the neighbourhood of interface is an effect of premature particle-matrix decohesion during crystallization. According to Rohatgi [5] the distribution of the fly ash particles is influenced by the tendency of particles to float due to density differences and interactions with the solidifying metal. He also pointed out that fly particles are present in the interdendritic regions between  $\alpha$ -Al dendrites due to lack of nucleation of  $\alpha$ -Al on fly ash particles and due to pushing on fly ash particles by growing  $\alpha$ -Al dendrites during solidification. Typical for all analysed composite structures is the presence of crushed fly ash precipitator particles, probably due to their high temperature treatment before incorporation into the melt and then vigorous mechanical stirring (Fig. 2b).

The diversified chemical composition of fly ash particles and its high reactivity can form compounds by chemical reactions between fly ash particles and liquid aluminium during the synthesis of the composites [17]. The reaction between fly ash-reinforcement containing silica and liquid aluminium can lead to the formation of alumina and silicon [17]:



In the ALFA composites after squeeze casting the influence of pressure on microstructure of materials may be noticed [3,9]. During crystallization pressure reduces the energy of the phase interaction at the liquid metal-solid particle boundary. Additionally, there is a high probability of occurrence of wettability (inherently related with the surface tension) of fly ash particles by molten alloy when external pressure is applied, whereas it does not occur in traditional gravity casting. These factors affect the good bond of fly ash particles with aluminium matrix (Fig. 3). Squeeze casting technique is favourable for obtaining a uniform distribution of reinforcement phase in the metal matrix [3,8]. External pressure applied on the melt during crystallization increases the cooling rate, the number of crystallization centres, solidification temperature ranges, and the rate of undercooling. It also decreases dendrite arm spacing, solidification time, critical radius of nuclei, changes in surface tension, specific volume, diffusivity and other parameters of crystallization [9]. These processes lead to a refining of structural components (particularly  $\alpha$ -Al+Si eutectic; see Figs. 3 and 4), the changes of distribution and character of the phases, different structural and chemical homogeneity and elimination of any kind of structural discontinuities (Fig. 3).

#### 4. Corrosion behaviour

Corrosion characteristics represented by corrosion, pitting and repassivation potentials (denoted by  $E_{\text{corr}}$ ,  $E_{\text{pit}}$  and  $E_{\text{rp}}$ , respectively) were determined from the electrochemical studies and analysis of anodic polarisation curves. Fig. 5 presents the polarisation curves of the studied materials in 3.5 wt.% aqueous solution, while the values of the potentials  $E_{\text{corr}}$ ,  $E_{\text{pit}}$  and  $E_{\text{rp}}$  are listed in Table 3. The additional electrochemical parameters, given in the table, are:  $\Delta E_{\text{pit}} = E_{\text{pit}} - E_{\text{corr}}$ , and  $\Delta E_{\text{rp}} = E_{\text{pit}} - E_{\text{rp}}$ . The parameter  $\Delta E_{\text{pit}}$  is a measure of the width of the passive region on the polarization curve and provides an indication of the susceptibility to pitting. The parameter  $\Delta E_{\text{rp}}$  is used to assess the repassivation behaviour of propagating pits and hence, the ease with which locally active sites can be eliminated.

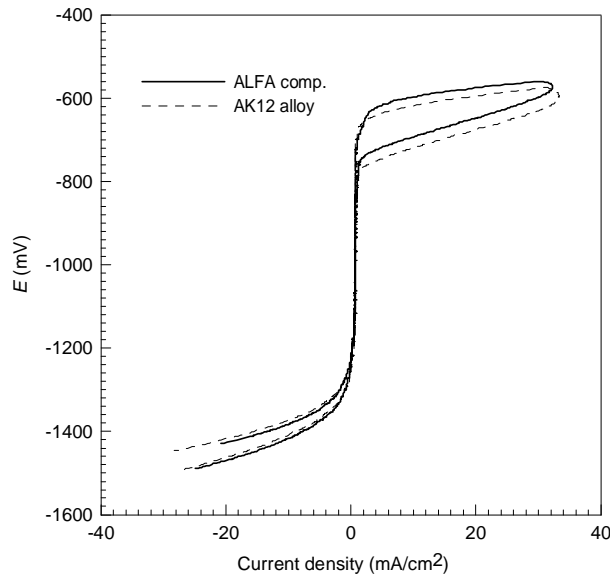


Fig. 5. Potentiodynamic polarization curves of the AK12/9.0% fly ash (75-100  $\mu\text{m}$  fraction) composite and AK12 alloy.

Table 3. Electrochemical data of AK12/9.0% fly ash (75-100  $\mu\text{m}$  fraction) composite and AK12 alloy from the corrosion testing.

Material	$E_{\text{corr}}$ (mV)	$E_{\text{pit}}$ (mV)	$E_{\text{tp}}$ (mV)	$\Delta E_{\text{pit}}$ (mV)	$\Delta E_{\text{tp}}$ (mV)
AK12-matrix alloy	-735	-613	-739	122	126
ALFA composite	-763	-640	-764	123	124

The nature of the potentiodynamic polarization curves in the 3.5% NaCl solution reveals typical characteristics of the metal undergoing spontaneous passivation. The shape of polarization curves (Fig. 5) and the determined electrochemical potentials of the ALFA composite and AK12 alloy are very similar. The corrosion potential  $E_{\text{corr}}$  value of the ALFA composite is lower (-763 mV) by 28 mV than that of the AK12 alloy (-735 mV), indicating that the former is more active than the latter. However, the pitting potential  $E_{\text{pit}}$  of the AK12 alloy is higher by a similar value than that of the ALFA composite. The slope of the linear sections of the anodic curves in relation to the  $x$ -axis above the  $E_{\text{pit}}$  point, together with a sudden increase in the current density, indicates rapid development of corrosion pits. The drop of corrosion current at the  $E_{\text{tp}}$  potential indicate that the pits cease to grow. The pits became repassivated and the corrosion is stopped. Repassivation potential  $E_{\text{tp}}$  for ALFA composite is lower than that for AK12 matrix alloy. More positive values of main electrochemical potentials for AK12 alloy indicate slightly higher corrosion resistance but they are not so significant. The electrochemical parameters  $\Delta E_{\text{pit}}$  and  $\Delta E_{\text{tp}}$  describing passivation and repassivation regions for both materials are almost identical (see Table 3).

Fig. 6 presents typical examples of the microstructure of the surfaces of samples after corrosion. In these cases crystallographic etching may be observed. The corrosion pits for both the ALFA composite (Fig. 6a and b) and matrix alloy AK12 (Fig. 6c) are formed in the solid solution  $\alpha$ -Al and in the neighbourhood of silicon. In the case of ALFA composite corrosion pits also occur in the interface of fly ash particles and matrix. In the microstructural images of the studied materials there are numerous pits of irregular shapes and depths ranging between 6 and 40  $\mu\text{m}$  for the ALFA composite and 8 and 50  $\mu\text{m}$  for the unreinforced aluminium alloy.

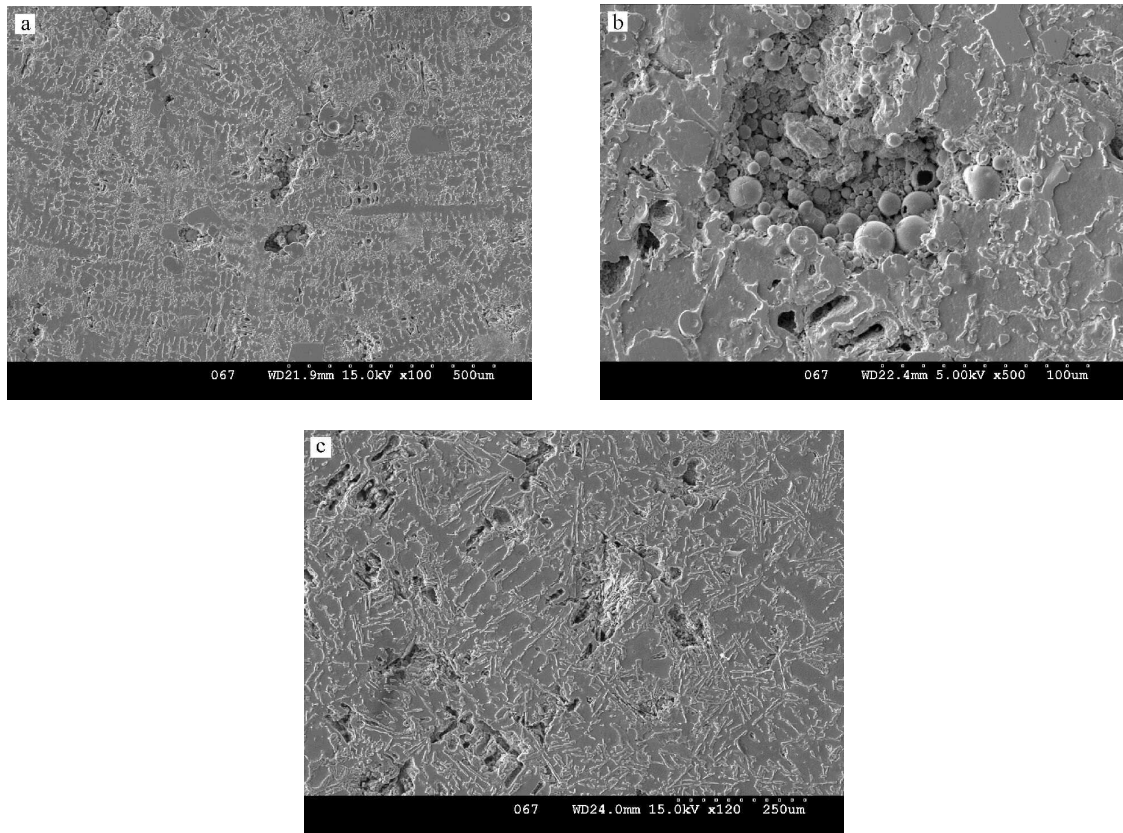


Fig. 6. Scanning electron micrograph of pitting corrosion on the surfaces of: (a, b) ALFA composites containing 9% wt. fly ash particles (75-100  $\mu\text{m}$  fraction) and (c) AK12 aluminium alloy.

Pitting corrosion appears mainly on metals and alloys in the passive state as a result of disarrangement of passive layer by aggressive environment elements (frequently  $\text{Cl}^-$  ions) on the heterogeneities of metals [18]. In the case of composites introduction of considerable amounts of alloy additions and reinforcing materials to the aluminium matrix releases intermetallic phases in the structure, which lead to the formation of galvanic couples favourable to corrosion. Moreover, factors influencing corrosion of the composites include porosity, segregation of alloying elements to the reinforcement/matrix interface, presence of an interfacial reaction product, high dislocation density around the reinforcement phase, voids at the reinforcement/matrix interface and electrical conductivity of the reinforcements [11,12].

The cathodic sites in the unreinforced alloy are eutectic silicon and/or intermetallic precipitates, whereas in the composites, depending on the composition of the alloy, the cathodic sites may be reinforcements second-phase precipitates, or the interfacial reaction products [19,20]. The presence of a very large number of second phase particles and mostly noble eutectic silicon, in general, in the composites leads to extensive pitting of the matrix and of the composites (Fig. 1). The incorporation of considerable amounts of alloy additions and reinforcing materials (reactivity of fly ash particles) to the aluminium matrix releases intermetallic phase in the structure, which results in the formation of „cathode patches” with good conductive properties of the passive layer. The presence of a more conductive phase at the interface provides an easier path for the electron exchange necessary for oxygen reduction and drives the anodic reaction at a higher rate in the MMC as compared to an aluminium alloy [21].

During the formation of MMCs intermetallic precipitates and segregation of alloying elements have been found to occur at the interface [21]. This prevents the formation of a continuous, resistive layer of aluminium oxide-reinforcement particles across the entire surface. From the point of

view of corrosion behaviour porosity observed in the composites microstructure is also important. During the corrosion process an increase in the concentration of aggressive  $\text{Cl}^-$  anions and  $\text{H}^+$  ions may occur in the pits and pores due to impeded replenishment of the solution. Due to the increase in the concentration of  $\text{Cl}^-$  and  $\text{H}^+$  ions passivation becomes difficult. Therefore, dissolution of metal in the pits is stimulated [18].

## 5. Corrosion kinetics

The results of the weight loss experiments as a function of corrosion time  $t$  are shown in Fig. 7. It may be seen from the figure that in the case of ALFA composite the weight loss regularly increases with time in the entire range of time up to 50 days. However, in the case of AK12 alloy the weight loss attains a constant value after about 25 days.

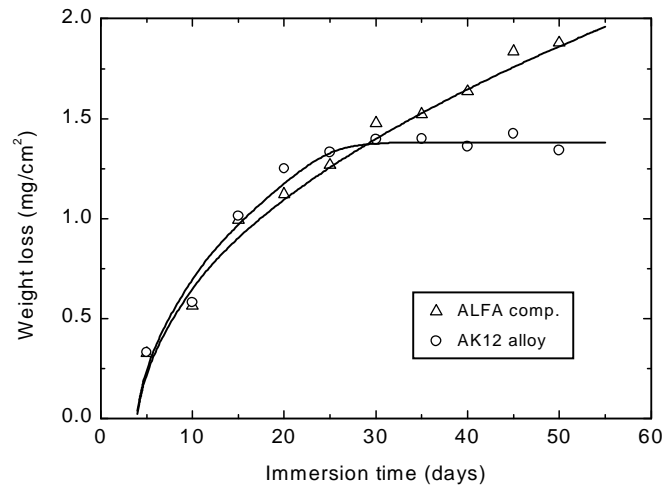


Fig. 7. Weight loss of AK12/9.0% fly ash (75-100  $\mu\text{m}$  fraction) composite and AK12 alloy immersed in open air 3.5 wt.% NaCl aqueous solution.

The time dependence of weight loss of the two samples, in the time interval when the weight loss increases with time, may be described by the following relations:

$$y = (a + bt)^{1/2}, \quad \text{parabolic law;} \quad (2)$$

$$y = k_1 \ln(k_2 + k_3t), \quad \text{logarithmic law;} \quad (3)$$

where  $y$  is the weight loss per unit area ( $\text{mg}/\text{cm}^2$ ),  $t$  is the time in days, and  $a$ ,  $b$  and  $k$ 's are constants. The values of the constants are given in Table 4.

Table 4. Values of constants of Eqs. (2) and (3).

Sample	Eq. (2)	Eq. (3)					
	$a$	$b$ ( $10^{-2} \text{ days}^{-1}$ )	$t^*$ (days)	$k_1$ ( $\text{mg}/\text{cm}^2$ )	$k_2$	$k_3$ ( $\text{days}^{-1}$ )	$t^*$ (days)
ALFA	-0.30	7.75	3.9	1.04	0.81	0.11	1.8
AK12	-0.35	8.68	4.0	0.65	0	0.31	3.3



It may be noted that for AK12 the two laws may be considered to be limiting laws, when the layer formed on the corroding surface attains a constant thickness. However, in the case of both samples, the two relations predict a threshold period  $t^*$  for the formation of a surface layer. By taking  $y = 0$  in Eqs. (2) and (3) one obtains the values of  $t^*$ , respectively, in the form:  $t^* = -a/b$ , and  $t^* = (1 - k_2)/k_3$ . These values of  $t^*$  are listed in Table 4.

It is well known [18,22] that corrosion of metals involves the formation of a surface film of an oxide phase separating the metal from the corroding reactant. Growth of the surface film takes place as a result of migration of the reactant through the surface film. If the oxide film formed on the surface is porous, corrosion continues until the whole of the metal is oxidized. However, if the oxide film is compact, adherent and pore-free, then it prevents the metal surface from subsequent oxidation. Compact, pore-free and adherent films formed on metals are usually thin while porous films are thick.

The above general ideas of corrosion of metals may be used to understand the corrosion kinetics of AK12 alloy and ALFA composite. As seen from Tables 1 and 2, AK12 alloy contains a lower Si content than ALFA composite. Therefore, the difference in their corrosion behaviour may be attributed to the difference in the Si content in the two samples, which results in the formation of oxide films of different compositions. The higher value of  $t^*$  for AK12 alloy suggests that this sample is more resistive to corrosion in the initial stages than ALFA composite (Table 4). This difference in the value of  $t^*$  may be attributed to the oxidation of silicon. However, as indicated by the values of  $b$  and  $k_3$ , after the threshold period  $t^*$  the corrosion of AK12 alloy occurs more rapidly than that of ALFA composite. The corrosion of AK12 alloy up to the limiting thickness implies that the oxide film formed on the surface is compact, adherent and pore-free and the main component of the oxide surface film contains silicon oxides. However, in the case of ALFA composite the oxide film is composed of a high amount of silicon oxides and is porous and thick.

Finally, it should be mentioned that the validity of Eq. (2) implies that corrosion of AK12 alloy and ALFA composite is controlled by the diffusion of reactant from the solution.

## 6. Conclusions

The following conclusions can be drawn from this study:

(1) Addition of fly ash particles as reinforcement in metal matrix composites and synthesis of ALFA composites by squeeze casting technology in comparison with gravity casting are advantageous for obtaining higher structural homogeneity with minimum possible porosity levels, good interfacial bonding and quite a uniform distribution of reinforcement.

(2) Fly ash particles lead to an enhanced pitting corrosion of the AK12/9.0% fly ash (75-100  $\mu\text{m}$  fraction) composite in comparison with unreinforced matrix (AK12 alloy). The enhanced pitting corrosion of ALFA composite is associated with the introduction of nobler second phase of fly ash particles, cast defects like pores, and higher silicon content formed as a result of reaction between aluminium and silica. The same factors (i.e. fly ash particles, cast defects and higher silicon content) also determine the properties of oxide film forming on the corroding surface.

## Acknowledgements

The authors express their gratitude Prof. K. Sangwal for his valuable advice and help in preparing the article.

The work was financed by State Committee for Scientific Research (grant No. 4 T08D 029 22).

## References

- [1] 1990 Coal Combustion By-Product., American Coal Ash Association, Revision No. 1, June 13, Washington D.C. (1992).

- [2] S. Nonavinakere, B. E. Reed, Proc. 10-th Intern. Ash Use Symp., Vol. 1, EPRI TR-101774, 1993, p. 120.
- [3] P. K. Rohatgi, R. Q. Guo, H. Iksan, E. J. Borchelt, R. Asthana, Mater. Sci. Eng. **A244**, 22-30 (1998).
- [4] T. Matsunaga, J. K. Kim, S. Hardcastle, P. K. Rohatgi, Mater. Sci. Eng. **A325**, 333 (2002).
- [5] P. K. Rohatgi, J. Met. **46**, 55-59 (1994).
- [6] K. Prabhakaran, K. G. K. Warriar, P. K. Rohatgi, Ceram. Int. **27**, 749 (2001).
- [7] P. K. Rohatgi, J. Sobczak, N. Sobczak, A. Karamara, S. Dybczak, Int. Conf. on Comp. Engin. ICCE-2, New Orleans, USA, 1995, p. 689-690.
- [8] P. K. Rohatgi, Z. Górny, J. Sobczak, N. Sobczak, Transactions of the Foundry Research Institute, **XLIII**(3), Kraków, 143-160 (1993).
- [9] J. Sobczak, Teoretyczne i praktyczne podstawy procesu prasowania w stanie ciekłym (squeeze casting) metali nieżelaznych (Theoretical and Practical Bases of Squeeze Casting of Non-ferrous Metals), Transactions of the Foundry Research Institute, Krakow (1993).
- [10] K. H. W. Seah, S. C. Sharma, B. M. Girish, Corrosion Sci. **39**, 2 (1997).
- [11] A. J. Trowsdale, B. Noble, S. J. Harris, I. S. R. Gibbins, G. E. Thompson, G. C. Wood, Corrosion Sci. **38**, 178 (1996).
- [12] R. L. Deuis, L. Green, C. Subramanian, J. M. Yellup, Corrosion **53**, 880 (1997).
- [13] L. H. Hihara, L. M. Latanision, Corrosion **48**, 546 (1992).
- [14] F. Mansfeld, S. Lin, S. Kim, H. Shih, J. Electrochem. Soc. **137**, 78 (1990).
- [15] J. Bieniaś, B. Surowska, Inż. Mater. **4**, 226 (2001).
- [16] P. K. Rohatgi, R. Guo, B. N. Keshavaram, D. M. Golden, Trans. Am. Foundrymen's Soc. **103**, 575-579 (1995).
- [17] R. Q. Guo, D. Venugopalan, P. K. Rohatgi, Mater. Sci. Eng. **A241**, 184 (1998).
- [18] G. Wranglén, Podstawy korozji i ochrony metali (An Introduction to Corrosion and Protection of Metals), WNT, Warszawa (1985).
- [19] P. Nunes, L. Ramanathan, Corrosion **51**, 615 (1995).
- [20] O. Modi, M. Saxena, B. Prasad, A. Jha, S. Das, A. Yegneswaran, Corrosion **54**, 133 (1998).
- [21] H. J. Greene, F. Mansfeld, Corrosion **53**, 922 (1997).
- [22] Z. Szklarska-Śmiałkowska, Pitting Corrosion of Metals, NACE, Houston (1986).